THE JOURNAL OF BIOLOGICAL CHEMISTRY VOL. 289, NO. 25, pp. 17515–17528, June 20, 2014

Caerulomycin A Enhances Transforming Growth Factor-β (TGF-β)-Smad3 Protein Signaling by Suppressing Interferon-γ (IFN-γ)-Signal Transducer and Activator of Transcription 1 (STAT1) Protein Signaling to Expand Regulatory T Cells (Tregs)*

Received for publication, December 24, 2013, and in revised form, April 21, 2014 Published, JBC Papers in Press, May 8, 2014, DOI 10.1074/jbc.M113.545871

Rama Krishna Gurram[1], **Weshely Kujur**[1], **Sudeep K. Maurya**[1], **and Javed N. Agrewala**[2]

From the Immunology Laboratory, Institute of Microbial Technology (Council of Scientific and Industrial Research), Chandigarh 160036, India

Background: Caerulomycin A, a known antifungal agent, was explored for its novel immunomodulatory activity.
Results: Caerulomycin A supports the generation of Tregs by augmenting the TGF-β-Smad3 and suppressing the IFN-γ-STAT1 signaling pathways by enhancing SOCS1 expression.
Conclusion: Caerulomycin A induces and enhances the Treg population.
Significance: Caerulomycin A can be a potent future drug for treating autoimmune diseases by eliciting the generation of Tregs.

Cytokines play a very important role in the regulation of immune homeostasis. Regulatory T cells (Tregs) responsible for the generation of peripheral tolerance are under the tight regulation of the cytokine milieu. In this study, we report a novel role of a bipyridyl compound, Caerulomycin A (CaeA), in inducing the generation of Tregs. It was observed that CaeA substantially up-regulated the pool of Tregs, as evidenced by an increased frequency of $CD4^+$ $Foxp3^+$ cells. In addition, CaeA significantly suppressed the number of Th1 and Th17 cells, as supported by a decreased percentage of $CD4^+$/IFN-γ^+ and $CD4^+$/$IL\text{-}17^+$ cells, respectively. Furthermore, we established the mechanism and observed that CaeA interfered with IFN-γ-induced STAT1 signaling by augmenting SOCS1 expression. An increase in the TGF-β-mediated Smad3 activity was also noted. Furthermore, CaeA rescued Tregs from IFN-γ-induced inhibition. These results were corroborated by blocking Smad3 activity, which abolished the CaeA-facilitated generation of Tregs. In essence, our results indicate a novel role of CaeA in inducing the generation of Tregs. This finding suggests that CaeA has enough potential to be considered as a potent future drug for the treatment of autoimmunity.

The immune system of the body is its artillery against pathogens. The immune response is very precisely tuned and tamed to discriminate self from non-self. Although the body does generate autoreactive T cells, the immune system has an accurate mechanism to eliminate such cells during thymic selection (1). Paradoxically, some autoreactive T cells can still escape deletion, establish themselves in the body, and become a potential threat to the host by generating autoimmune diseases. The body has developed additional defense mechanisms against these treacherous cells through the induction of peripheral tolerance, anergy/unresponsiveness, release of immunosuppressive molecules (TGF-β, IL-10, IL-35, etc.), and generation of regulatory T cells (Tregs)[3] (2–4). Despite extremely careful mechanisms operating in the body to safeguard against autoreactive T cells, these cells may still become activated and can be terrifically devastating in inflicting injury by causing autoimmune diseases (5).

Autoimmune diseases can be treated by non-steroidal anti-inflammatory drugs, corticosteroids, disease-modifying anti-rheumatic drugs, and immunosuppressive agents (6). However, the limitations and side effects associated with the use of these drugs pave the way toward better and safer remedial measures (7–9). Recently, the generation of antigen-specific tolerance by Tregs has gained considerable impetus following the observation that these cells are endowed with enough potential to suppress autoimmune reactions (10, 11).

Tregs are a subset of $CD4^+$ helper T cells that specifically express fork head family transcription factor 3 (Foxp3) (12, 13). Recently, several strategies have been undertaken to enhance the production of Tregs for treating autoimmune diseases (14, 15). Naïve $CD4^+$ T cells can be differentiated into Tregs by TGF-β (16). Furthermore, Tregs can be increased by antagonizing TNF-α activity (17). Interestingly, it has also been reported that rapamycin (Rapa), an immunosuppressive drug, can successfully expand Tregs (18). Additionally, LY294002 is also known to induce Tregs (19). Unfortunately, Rapa increases the chance of diabetes (20).

It is a well known fact that most of the revolutionary medicines, like Rapa, cyclosporin A, and FK506, exhibiting antibiotic

* This work was supported by the Council of Scientific and Industrial Research.
[1] Recipient of fellowships of the Council of Scientific and Industrial Research, New Delhi, India.
[2] To whom correspondence should be addressed: Immunology Laboratory, Institute of Microbial Technology (Council of Scientific and Industrial Research), Sector 39A, Chandigarh 160036, India. E-mail: javed@imtech.res.in.

[3] The abbreviations used are: Treg, regulatory T cell; Rapa, rapamycin; CaeA, Caerulomycin A; Ab, antibody; qPCR, quantitative PCR.

or antifungal properties were later proven to possess potent immunosuppressive activity (21–23). CaeA is a bipyridyl compound and has been reported in the literature to show antifungal and antibiotic properties (24, 25). Hence, it encouraged us to study whether CaeA could also exhibit immunosuppression, in particular by evoking the generation of Tregs, as observed in the case of Rapa (18).

In this study, we have shown that CaeA independently induced Tregs (cTregs) and synergistically supported the TGF-β-mediated expansion of Tregs (cβTregs). We also revealed the mechanism of action involved in the generation of Tregs by CaeA. Finally, the proof of concept was established by successfully treating animals suffering from arthritis with CaeA.

EXPERIMENTAL PROCEDURES

Mice—Female C3He and BALB/c mice and male DBA/1 mice 6–8 weeks of age were procured from the experimental animal facility of the Institute of Microbial Technology. The study was approved by the Institutional Animal Ethical Committee.

Chemicals and Antibodies—The chemicals and reagents were procured from Sigma-Aldrich (St. Louis, MO) or as mentioned otherwise. RPMI 1640, FBS, and TRIzol reagent were procured from Invitrogen. Penicillin, streptomycin, and pyruvic acid were from Serva (Heidelberg, Germany). Phosphatase inhibitor mixture, STAT1, and Smad3 oligo were from Santa Cruz Biotechnology (Dallas, TX). CaeA was from LKT Laboratories (St. Paul, MN). Anti-phospho-STAT1, anti-phospho-STAT3, anti-phospho-STAT4, and anti-phospho-STAT6 and total STAT1, STAT3, STAT4, and STAT6 were from BD Biosciences. Anti-phospho-Smad3 and total Smad3, Smad7, and JAK1 Abs were from Abcam (Cambridge, MA). Anti-JAK2 Ab and protein G-agarose beads were from Cell Signaling Technology (Danvers, MA).

Medium—All the experiments were carried out in RPMI 1640 supplemented with penicillin (70 mg/liter), streptomycin (100 mg/liter), $NaHCO_3$ (2.2 g/liter), HEPES (2.38 g/liter), pyruvic acid (110 mg/liter), and FBS (10%).

In Vitro Th Cell Differentiation—Naïve CD4 T cells (2×10^5/ml) were stimulated using plate-bound anti-CD3 Ab (2 μg/ml) and soluble anti-CD28 Ab (1 μg/ml) along with following polarizing conditions to differentiate them in to different Th subsets. Tregs were generated by providing the polarizing conditions using TGF-β: 5 ng/ml + IL-2: 100 units/ml for 5 days; Th1 cells by incubating with IL-12: 5 ng/ml + anti-IL-4 Ab: 10 μg/ml + IL-2: 100 units/ml for 4 days; Th17 cells by culturing with IL-6: 40 ng/ml + TGF-β: 2.5 ng/ml + anti-IL-4 Ab: 10 μg/ml + anti-IFN-γ Ab: 10 μg/ml for 4 days. In case of Th1 and Th17 cells, media supplemented with their respective polarizing cytokines were replenished and cells were cultured for additional 2 days. The purity of Tregs, Th1, and Th17 was measured by intracellular expression of Foxp3, IFN-γ, and IL-17, respectively. Before harvesting from the cultures, Th1 and Th17 cells were treated with phorbol 12-myristate 13-acetate (40 nM) and ionomycin (1 μM) for 2 h. To block cytokine secretion, brefeldin A (10 μg/ml) was added. Later, and cells were incubated further for 3 h. Tregs, Th1, and Th17 cells were cultured with different concentrations of CaeA (0–0.15 μM). The modulation in the frequency of Tregs, Th1, and Th17 cells was analyzed by flow cytometry.

Treg Functional Assay—CD4 T cell activation was performed as described elsewhere (26). Briefly, CD4 T cells (2×10^5 cells/200 μl) were stimulated with anti-CD3 and CD28 Abs. Tregs were added to the cultures and incubated for 48 h. Later, cells were harvested and studied for activation by flow cytometry.

An alloresponse experiment was performed using splenocytes (2×10^5) of MHC-mismatched strains of mice. The C3He (H-2^k) cells served as the responder and γ-irradiated DBA/1 (H-2^q) cells as the stimulator. Alloresponse cultures were set in the presence or absence of Tregs for 4 days. Later, cultures were pulsed with 1 μCi of [*methyl*-^{3}H] thymidine for 16 h. The cells were harvested onto glass filter mats, and incorporated radioactivity was measured as counts per minutes by scintillation counting.

Generation of the Experimental Arthritis Model and Disease Assessment—The induction of arthritis and disease symptoms were monitored as described previously (27). Briefly, male DBA/1 mice (6 mice/group) were immunized intradermally on day 0 with bovine collagen type II (100 μg) emulsified in complete Freund adjuvant (4 mg/ml desiccated *Mtb H37Ra*). A booster dose of bovine collagen type II in incomplete Freund adjuvant was injected on day 21. Later, CaeA (1 and 10 mg/kg body weight) and 0.5% carboxyl methyl cellulose emulsion in water was administered daily for 50 days, and animals were monitored every day for arthritis symptoms. A group treated with carboxyl methyl cellulose (0.5%) was taken as a vehicle control (placebo). Disease progression was assessed for a clinical score using following criteria: 0, no symptoms; 1, mild erythema and inflammation in the limb digits; 2, severe inflammation up to the paw; and 3, severe inflammation up to the ankle region. These score norms were adopted for each limb.

For immunological assays, animals were sacrificed on day 30. The optimum response was reported during that period (28). The cells isolated from the lymph nodes were pooled and *in vitro*-challenged with bovine collagen type II (50 μg) for 72 h. Later, proinflammatory cytokines (IFN-γ and TNF-α) in the culture supernatants were measured by ELISA according to the instructions of the manufacturer. The proinflammatory markers matrix metalloproteinase-3 in the serum and IL-6, TNF-α, and IFN-γ in the knee joints were estimated on day 50. For histopathological analysis, the knee joints were fixed in buffered formalin (10%) and decalcified in formic acid (1%). Microtome sections of paraffin-embedded knee joints were stained with H&E to observe the extent of inflammation.

Fluorescence Imaging—The fluorescence imaging of arthritis-induced mice was performed with the help of the *in vivo* imager FMT 2500 Lx (PerkinElmer Life Sciences, Waltham, MA). ProSense 680 and 750 (cathepsin-specific activatable probes) and OsteoSense 680 and 800 (specific for bone degeneration) were used for visualizing inflammatory responses. These reagents were injected intravenously 24 h prior to imaging. Later on, hairs were removed by hair clipper and depilatory cream. The animals were imaged under a given laser wave length for excitation (680, 750, and 780 nm) and emission fluorescence (700, 780, and 805 nm). All procedures were per-

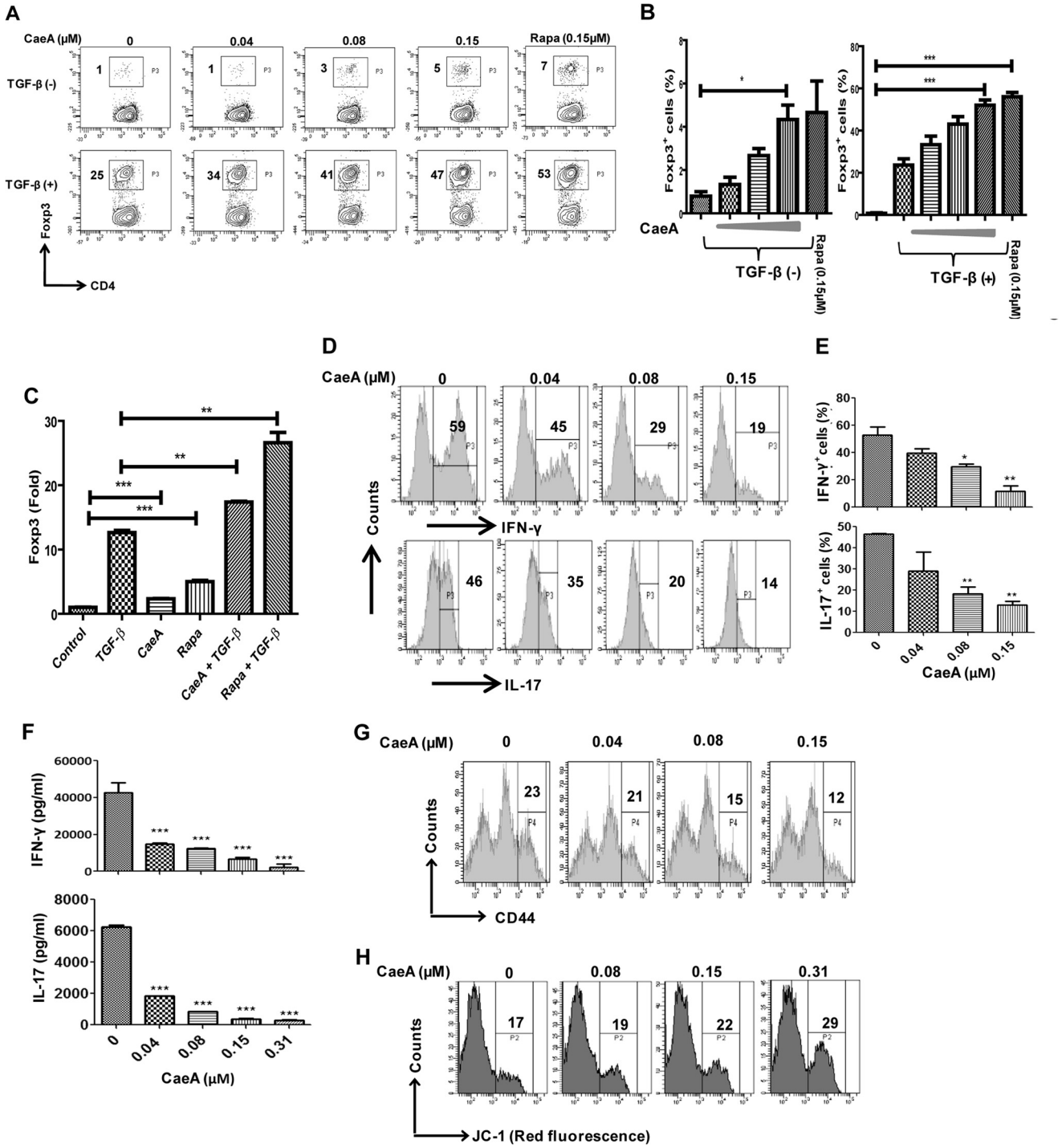

FIGURE 1. **CaeA alone and in conjunction with TGF-β augments the pool of Tregs.** Naïve CD4 T cells stimulated with anti-CD3 and CD28 Abs were incubated with either Tregs or Th1 or Th17 polarization conditions and different concentrations of CaeA. The cells were analyzed for the expression of Foxp3, IFN-γ, and IL-17 to monitor the frequency of Tregs, Th1, and Th17, respectively. *A*, the augmented population of Foxp3$^+$ CD4 T cells is indicated by the percentage in the *insets* of the flow cytometry contour plots. *B*, Data are mean ± S.E. *C*, fold change by RT-qPCR. Rapa is used as a positive control. *D*, the decline in the yield of IFN-γ and IL-17 by CaeA treatment is depicted by the percentage in the *insets* of the flow cytometry histograms. *E*, data are mean ± S.E. *F*, picograms/milliliters estimated through ELISA. *G*, flow cytometry histograms depicting the decrease in CD44 expression. *H*, the increase in mitochondrial membrane potential on CaeA treatment. The control cultures comprises cells incubated with medium alone (no CaeA or TGF-β) or in the presence of TGF-β alone (no CaeA). *, $p < 0.05$; **, $p < 0.005$; ***, $p < 0.0001$. The results shown are from three to five independent experiments.

formed under gas anesthesia (isoflurane). The intensity of fluorescence was directly proportional to the severity of the disease. Image processing and analysis was performed by TrueQuant software.

Isolation of Naïve CD4$^+$ T Cells—CD4$^+$ T cells were isolated by magnetic activated cell sorting according to the instructions of the manufacturer (CD4 T cell enrichment kit, BD Biosciences). Briefly, splenocytes obtained from two mice were

pooled and RBC-depleted by ACK (ammonium-chloride-potassium) lysis buffer. Later, the cells were incubated with CD4 T cell enrichment mixture (50 μl/10^7 cells) and biotin anti-CD25 Ab (5 μl/10^7 cells) for 30 min at 4 °C. The unbound Abs were removed by washing with RPMI 1640 (400 g, 5 min). The residual pellet was incubated with BD™ IMag streptavidin particles plus-DM (50 μl/10^7 cells) for 30 min at 4 °C. The cells were suspended in 4 ml of RPMI and placed in contact with iMagnet for 8 min. The $CD4^+$ T cells obtained by negative selection were of 92% purity, as confirmed by flow cytometry.

Real-time PCR—RNA from the cell pellet or tissue sample was isolated using TRIzol reagent according to the instructions of the manufacturer. Isolated RNA was reverse-transcribed to cDNA with the help of a cDNA synthesis kit. cDNA was analyzed for the expression of Foxp3, Smad7, T-bet, SOCS1, ISG15, IRF-1, IRF-7, TNF-α, IFN-γ, and IL-6 by a Quantifast SYBR Green PCR kit with the help of a Realplex master cycler (Eppendorf, Hamburg, Germany). The following sequences were used: T-bet, 5′-CTAAGCAAGGACGGCGAAT-3′ (forward) and 5′-TTCCACACTGCACCCACTT-3′ (reverse); TNF-α, 5′-GAACTGGCAGAAGAGGCACT-3′ (forward) and 5′-AGGGTCTGGGCCATAGAACT-3′ (reverse); Foxp3, 5′-TTCATGCATCAGCTCTCCAC-3′ (forward) and 5′-CTGGACACCCATTCCAGACT-3′ (reverse); IFN-γ, 5′-TGAACGCTACACACTGCATCTT-GG-3′ (forward) and 5′-CGACTCCTTTTCCGCTT-CCTGAG-3′ (reverse); β-actin, 5′-AGAGGGAAATCGTGCGTGAC-3′ (forward) and 5′-CAATAGTGATGACCTGGCCGT-3′ (reverse); Smad7, 5′-AAGTGTTCAGGTGGCCGGATC-TCAG-3′ (forward) and 5′-ACAGCATCTGGACAGC-CTGCAGTTG-3′ (reverse); SOCS1, 5′-ACCTTCTTGGTGCGCGAC-3′ (forward) and 5′-AAGCCATCTTCACGCTGAGC-3′ (reverse); IRF1, 5′-CAGAGGAAAGAGAGAAAGTCC-3′ (forward) and 5′-CACACGGTGACAGTGCTGG-3′ (reverse); IRF7, 5′-CTGGAGCCATGGGTATGCA-3′ (forward) and 5′-AAGCACAAGCCGAGACTGCT-3′ (reverse); and ISG15, 5′-GGAACGAAAGGGGCCACAGCA-3′ (forward) and 5′-CCTCCATGGGCCTTCCCTCGA-3′ (reverse). Ct values of experimental samples were normalized against β-actin, and analysis was done by comparative Ct method. Results are represented in the form of relative expression (fold).

ELISA—The cytokines IFN-γ, TNF-α, and IL-17 secreted in the culture supernatants were determined by sandwich ELISA. Briefly, ELISA plates were coated with the appropriate concentration of specific Ab in phosphate buffer (pH 9.2) for 12 h at 4 °C. Later, the plates were blocked with BSA (1%) to eliminate nonspecific binding. ELISA plates were incubated with culture supernatants and appropriate standards for 12 h at 4 °C. The plates were treated with respective biotin-conjugated secondary Abs, followed by streptavidin-HRP. The plates were developed with the help of the substrate H_2O_2 and the chromogenic agent *O*-phenylenediamine. The optical density of color development was measured at 495 nm. Each step was followed by washing five times with 1× PBS-Tween 20 (0.05%) and regular incubation steps. The level of cytokines was estimated by plotting a standard curve using recombinant cytokines and expressed as picograms/milliliter.

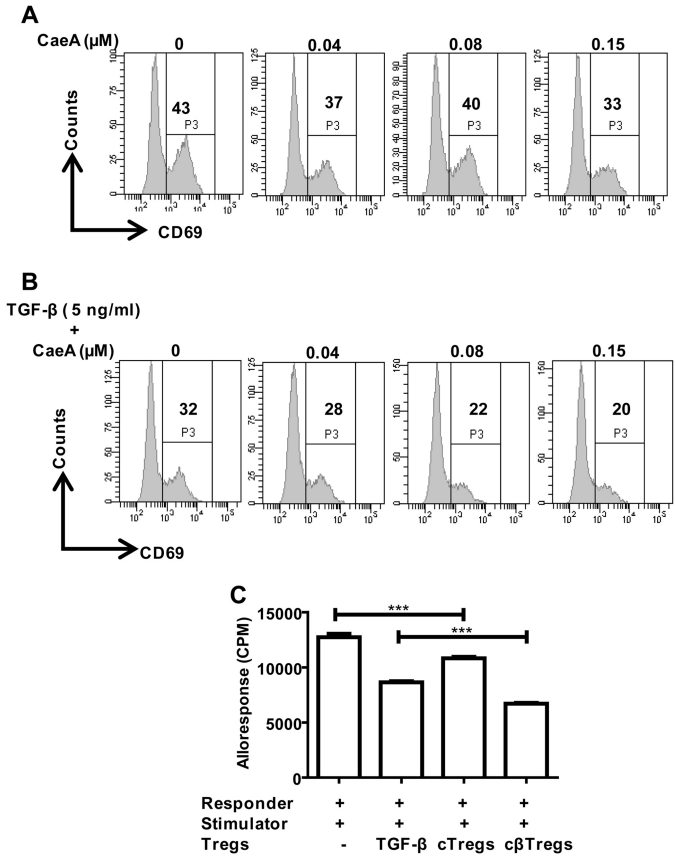

FIGURE 2. **Tregs generated in the presence of CaeA suppress the activation and function of CD4 T cells.** Tregs generated with the indicated concentrations of CaeA and in the absence (*A*) and presence (*B*) of TGF-β were cultured with effector CD4 T cells (*A* and *B*) and alloreactive T cells (*C*). *A* and *B*, the *insets* of the flow cytometry histograms depict the percentage of $CD4^+$/$CD69^+$ T cells. *C*, bar diagram representing proliferation as mean ± S.D. of the radioactivity incorporated (counts per minute, *CPM*) in alloreactive T cells. ***, $p \leq 0.0001$. The results are from two to three independent experiments.

EMSA—The IFN-γ-mediated STAT1 response was measured by initially incubating CD4 T cells with CaeA (0–0.31 μM) for 24 h, followed by IFN-γ (200 units/ml) stimulation for 30 min. To evaluate the TGF-β-mediated Smad3 response, CD4 T cells were incubated initially with CaeA (0–0.31 μM) for 24 h, followed by IFN-γ (200 units/ml) treatment for 48 h. Later, cells were pulsed with TGF-β (2 ng/ml) for 1 h. As a positive control for STAT1 suppression, cells were also cultured with the JAK inhibitor pyridone 6. Immediately thereafter, the nuclear extract was prepared, and EMSA was performed, as described elsewhere (29). Briefly, the nuclei of cells were isolated by suspending cells in hypotonic conditions in buffer A (20 mM HEPES (pH 7.4), 0.42 M NaCl, 1.5 mM $MgCl_2$, 0.2 mM EDTA, and 25% glycerol) containing the following proteinase inhibitors: 0.5 mM dithiothreitol, 1 mM PMSF, 2 μg/ml leupeptin, and 10 μg/ml aprotinin. Nuclear proteins were extracted in buffer B (20 mM HEPES (pH 7.4), 50 mM KCl, 0.2 mM EDTA, 20% glycerol, and proteinase inhibitors) and used for analysis of DNA binding. The double-stranded oligonucleotide of the consensus sequences 5′-CATGTTATGCATATTCCTGTAAGTG-3′ (STAT1) and 5′-TCGAGAGCCAGACAAAAAGCCAGACATTTAGCCAGACAC-3′ (Smad3) was used for EMSA. The double-stranded oligo was end-labeled

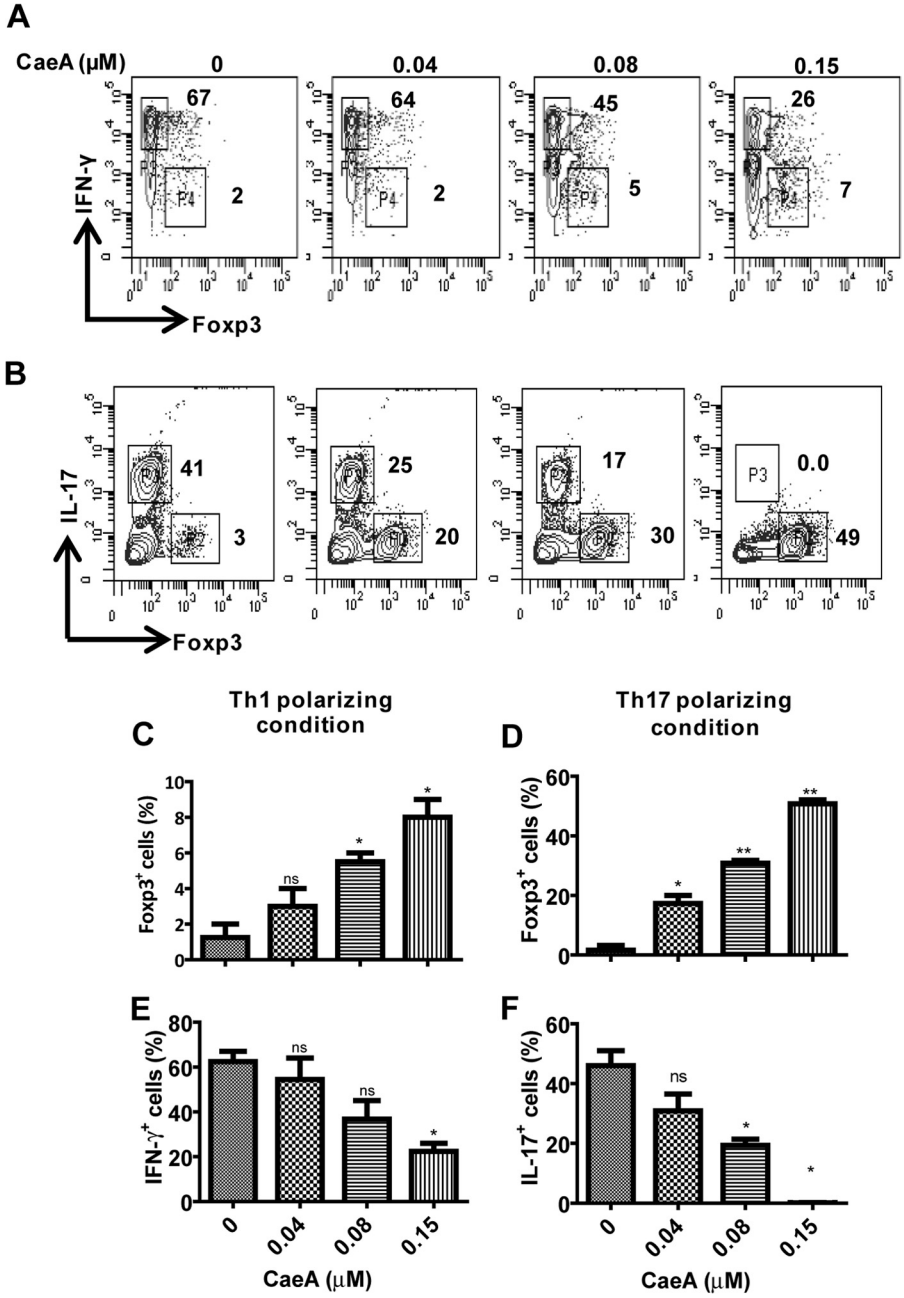

FIGURE 3. **CaeA-induced Treg expansion is not influenced by Th1 and Th17 polarizing conditions.** Anti-CD3 and CD28 Ab-stimulated naïve CD4 T cells were cultured under either Th1 (*A*) or Th17 (*B*) polarizing conditions with the indicated concentrations of CaeA. *A*, the data in the *insets* of the flow cytometry contours depict an enhanced percentage of Foxp3$^+$ cells *versus* IFN-γ^+ (*A*) and IL-17$^+$ (*B*) CD4 T cells. *C* and *D*, bar diagram representing mean ± S.E. and indicating an increase in the percentage of CD4$^+$/Foxp3$^+$ T cells under Th1 and Th17 polarizing conditions, respectively. *E* and *F*, a decrease in the percent population of CD4$^+$ T cells expressing IFN-γ and IL-17 intracellularly. The results shown are from three independent experiments. *, $p < 0.05$; **, $p < 0.005$; *ns*, not significant.

with [γ-^{32}P]ATP with the help of T4 polynucleotide kinase. The binding reaction was carried out for 30 min at room temperature using nuclear extract (5 μg) along with a labeled probe in a final volume of 20 μl of buffer (10 mM Tris (pH 7.5), 0.1 mM EDTA, 5 mM $MgCl_2$, 80 mM KCl, 0.8 mM dithiothreitol, 2.5% glycerol, and 1 μg of poly(dI-dC)). The protein with the DNA complex was separated in polyacrylamide gel (4%) using Tris borate-EDTA buffer. After electrophoresis, the gel was dried and exposed to the imager screen at room temperature for 12 h and scanned using a PhosphorImager (Fujifilm, Tokyo, Japan).

Immunoprecipitation—CD4$^+$ T cells pulsed with IFN-γ for 15 min were lysed in radioimmune precipitation assay buffer. The whole cell lysate was precleared using normal rabbit serum and protein G-agarose beads for 1 h at 4 °C. Later, protein G-agarose beads were separated from the lysate by centrifugation (5000 × *g*, 5 min). The cell lysate was then incubated with either anti-JAK1 or JAK2 Abs overnight at 4 °C. Protein G-agarose beads were added and incubated for 1 h at 4 °C. The immune complexes were isolated by centrifugation (5000 × *g*, 5 min). Purified complexes were boiled in SDS sample buffer and

used to analyze the phosphorylation of JAK1 and JAK2 proteins by Western blotting.

Western Blotting—The expression of Smad7 and T-bet and the phosphorylation of STAT1, STAT3, STAT4, Smad3, JAK1, and JAK2 were analyzed by Western blotting. Briefly, the whole cell lysate was prepared by suspending cells in radioimmune precipitation assay buffer. The protein concentration was estimated by Bradford assay. The equal concentration of protein

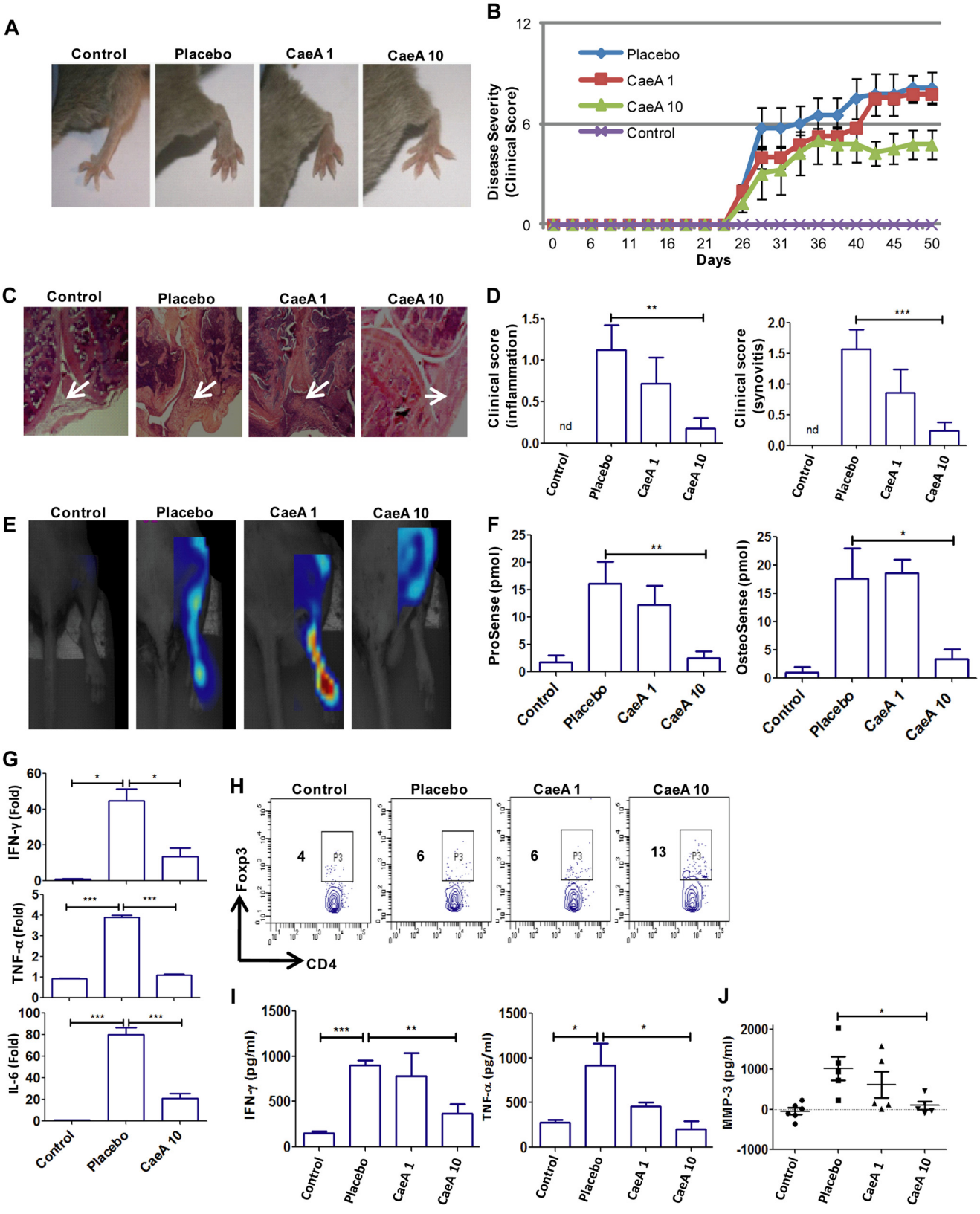

lysate of all samples was separated on SDS-PAGE gels (12%) followed by transfer to a nitrocellulose membrane at 4 °C for 12 h. Membrane transfer was followed by blocking with BSA (5%) in PBS and then probing with their specific Abs, followed by HRP-conjugated secondary Abs. The blots were visualized by ECL Plus Western blotting substrate. The blots were developed onto x-ray film (Amersham Biosciences Hyperfilm ECL, GE Healthcare). Internal loading was analyzed by stripping off the primary Ab and reprobing with a suitable Ab.

Mitochondrial Membrane Potential Analysis—CD4 T cells stimulated with anti-CD3 (2 μg/ml) and CD28 (1 μg/ml) Abs were cultured with CaeA (0–0.31 μM) for 72 h. Later, cells were pelleted and resuspended in JC-1 (5,5′,6,6′-tetrachloro-1,1′,3,3′-tetraethylbenzimidazolylcarbocyanine iodide) medium (2.5 μg/ml). The cultures were incubated at room temperature for 15–20 min in the dark. Later, cells were washed with flow cytometry staining buffer (2% FBS in PBS) and acquired immediately using a flow cytometer (FACSCalibur), and then the analysis was done using FACSDiva software. The increase in the mitochondrial membrane potential was measured by the change in the fluorescence intensity of JC-1 from a green to a red wavelength.

Flow Cytometry—The cells were harvested from the cultures and washed with flow cytometry buffer (PBS and 2% FBS). The Fc receptor was blocked by using anti-CD16 Ab, followed by staining with fluorochrome-conjugated anti-CD4 and CD69 Abs and their respective isotype-matched control Abs for 30 min at 4 °C. For staining with biotinylated Abs, cells were incubated with biotin-conjugated Abs for 30 min at 4 °C, followed by incubation with fluorochrome-conjugated streptavidin. Finally, cells were washed and fixed in paraformaldehyde (1%). Intracellular cytokine staining was performed by first staining for surface markers followed by fixing with paraformaldehyde (4%) for 20 min at 4 °C. Later, the cells were washed twice in staining buffer and resuspended in permeabilizing buffer (1× PBS/0.1% saponin/1% FBS) at room temperature for 20 min. This was followed by incubating with appropriate Abs or their isotype-matched controls for 30 min. Cells were washed twice with permeabilizing buffer and resuspended in staining buffer. Nuclear protein Foxp3 staining was performed with a Foxp3 buffer staining kit according to the instructions of the manufacturer (eBioscience, San Diego, CA). Cells were acquired using FACSCalibur or FACSAria II. Analysis was performed by FACSDiva software.

Statistical Analysis—Statistical analysis was performed with the help of GraphPad Prism software. The differences between groups were compared by statistical analysis (two-tailed, unpaired Student's *t* test).

RESULTS

Induction of the Enhancement of Foxp3$^+$ CD4 T Cells by CaeA—The expression of Foxp3 is crucial for the generation of Tregs. Rapa is a known immunosuppressive drug that has been reported to induce Treg formation (18). Hence, in the preliminary phase of the study, we tested whether CaeA can elicit the generation of Tregs. Interestingly, we observed that anti-CD3 and CD28 Ab-stimulated naïve CD4$^+$ T cells cultured with CaeA showed a significant ($p < 0.05$) increase in Foxp3$^+$ T cells (cTregs) (Fig. 1*A*). Further, supplementing cultures with TGF-β significantly ($p < 0.005$) promoted the pool of Foxp3$^+$ CD4 T cells (cβTregs) (Fig. 1, *A* and *B*). The enhancement in the frequency of Foxp3$^+$ CD4 T cells was observed in a dose-dependent fashion. The data were reproduced by both flow cytometry and RT-qPCR (Fig. 1 C). The results were comparable with Rapa, which was used as a positive control (Fig. 1, *A*–*C*). We also noticed an up-regulation of CD25 (IL-2 receptor) expression on CD4 T cells on CaeA treatment, which was augmented further on complementing the cultures with TGF-β (data not shown). Intriguingly, naïve CD4 T cells cultured with CaeA under Th1 and Th17 polarizing conditions exhibited a significant decline in the expression ($p < 0.005$) and secretion ($p < 0.0001$) of IFN-γ and IL-17 by CD4 T cells, respectively (Fig. 1, *D*–*F*). Furthermore, down-regulation of CD44 and an increased mitochondrial membrane potential was noticed in CD4 T cells on treatment with CaeA (Fig. 1, *G* and *H*). T cell activation (CD44^{hi}) is inversely proportional to the mitochondrial membrane potential (30). We observed a similar effect with CaeA.

Tregs Generated in the Presence of CaeA Significantly Suppressed the Activity of Effector T Cells—We next checked whether cTregs and cβTregs were capable of inhibiting the function of effector T cells. It is noteworthy that a diminished expression of CD69 was observed on effector CD4 T cells cocultured with either cTregs or cβTregs (Fig. 2, *A* and *B*). Further, cTregs and cβTregs substantially ($p < 0.0001$) retarded the alloresponse in a mixed lymphocyte reaction (Fig. 2 C). However, the extent of suppression was better in the case of cβTregs than cTregs. These data clearly signify that cTregs and cβTregs are functionally active and have the potential to retard the activity of effector T cells.

CaeA Sufficiently Expands Foxp3$^+$ Tregs under Th1 and Th17 Polarization Conditions—Loss of Tregs is one of the main reasons for the breakdown of peripheral tolerance. The instability of Tregs under proinflammatory conditions is a major hurdle for the restoration of tolerance by reprogrammed Tregs

FIGURE 4. **CaeA ameliorated the symptoms of experimental arthritis by generating Tregs.** Arthritis-induced mice were treated with CaeA. *A*, disease progression/regression was monitored by clinical symptoms, as indicated under "Experimental Procedures." Photos of the hind limbs only show inflammation and swelling. *B*, line diagram representing the severity of disease on the basis of the clinical score (0, no symptoms; 1, mild erythema and inflammation in the digits; 2, severity of inflammation up to the paw; and 3, severity of inflammation up to the ankle region). *Error bars* indicate the mean ± S.E. *C*, histopathology data representing H&E-stained sections of knee joints, showing decreased cell infiltration in the joint cavities of CaeA-treated animals. *D*, bar diagram indicating a decrease in inflammation and synovitis by CaeA (nd, not detected). *E*, fluorescent tomographic imaging of hind limbs probed with ProSense 680, signifying a decrease in disease severity by CaeA treatment. *F*, bar diagram representing the quantification of inflammation in picomoles in the hind limbs using ProSense and OsteoSense. *G*, RT-qPCR data representing the fold change in the level of cytokines in the knee joints of animals. *H*, data in the *insets* of the flow cytometry contour plots depict the increased percentage of CD4 T cells expressing Foxp3 on CaeA treatment. *I*, ELISA data of cytokines are expressed as picograms/milliliter and depict the decreased yield of IFN-γ and TNF-α on treatment with CaeA. *J*, levels in picograms/milliliter of MMP-3 in serum as measured by ELISA. The results shown are from two to three independent experiments with 5–6 mice/group. *, $p \leq 0.05$; **, $p \leq 0.005$; ***, $p \leq 0.0001$.

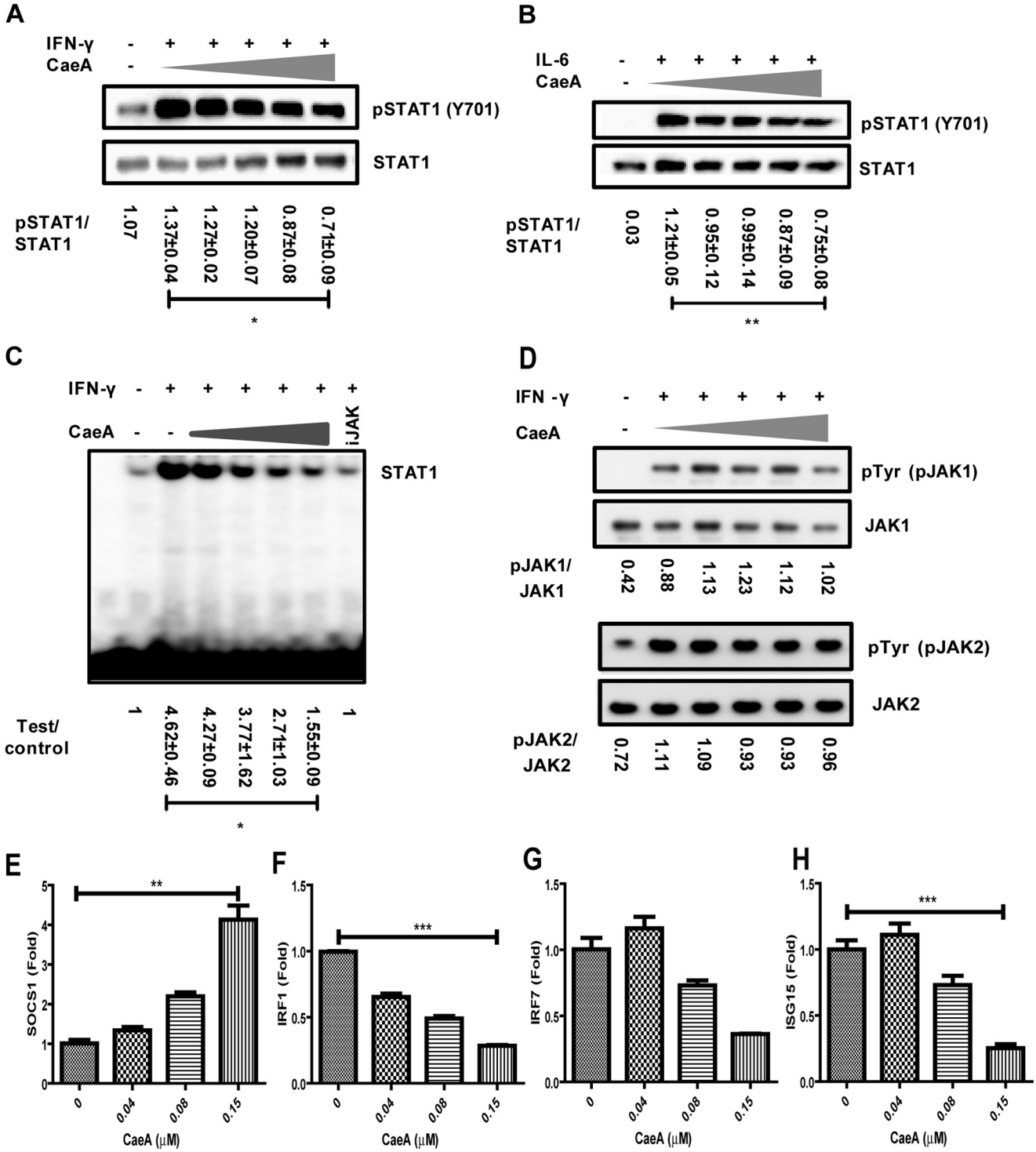

FIGURE 5. **CaeA antagonized the IFN-γ- and IL-6-mediated STAT1 signaling pathway in CD4 T cells by enhancing SOCS1 expression.** CD4 T cells were treated with various concentrations of CaeA (0.04–0.31 μM) for 24 h prior to the stimulation with IFN-γ (*A* and *C*) and IL-6 (*B*) for 15 min. *A* and *B*, phosphorylation of STAT1 was analyzed by Western blotting. *C*, nuclear translocation by EMSA. The last lane indicating the inhibitor of JAK (*iJAK*) represents pyridone 6, the positive control for STAT1 inhibition. *D*, Western blot images designating the phosphorylation of JAK1 and JAK2. The data in the *insets* of the figures represent the fold change in phosphorylation (*A*, *B*, and *D*) and nuclear translocation (*C*). RT-qPCR data represented as bar diagrams (mean ± S.E.) illustrate the expression of SOCS1 (*E*), IRF1 (*F*), IRF7 (*G*), and ISG15 (*H*). The results shown are from three independent experiments. *, $p \leq 0.05$; $p \leq 0.005$; ***, $p \leq 0.0001$.

(31). Hence, proinflammatory conditions reciprocally regulate Treg generation by favoring pathogenic Th17 cell development (32). Hence it was crucial for us to monitor whether the presence of Th1 and Th17 polarizing cytokines can influence the differentiation of CaeA-induced Tregs. It is of interest to note that the proinflammatory milieu could not change the generation of Tregs (Fig. 3, *A*–*D*). In contrast, a significant reduction was observed in the frequency of IFN-γ- and IL-17-producing

T cells (Fig. 3, *E* and *F*). The response was observed to be in a dose-dependent manner (Fig. 3, *A–F*). The data denote that the presence of the Th1 and Th17 differentiation cytokines IFN-γ and IL-17, respectively, does not hinder the CaeA-induced formation of Tregs.

CaeA Ameliorates Clinical Symptoms in an Experimental Model of Arthritis—Th1 and Th17 cells play a potential role in the progression of autoimmune diseases (33). In contrast, Tregs are known to suppress autoimmunity (34). Because cTregs suppress both Th1 and Th17 cells, it was obvious to check whether the administration of CaeA can restrain autoimmunity. In this study, we used a collagen-induced animal model of arthritis. Fascinatingly, there was a regression in the clinical symptoms of arthritis upon treatment with CaeA (Fig. 4*A*). The animals were monitored for a clinical score over a period of 50 days (Fig. 4*B*). Furthermore, this observation was supported by the histopathological examination, which revealed decreased infiltration and less synovitis of the joint capsule of animals treated with CaeA (Fig. 4, *C* and *D*). Furthermore, we substantiated our finding by examining decreased inflammation by employing a whole body fluorescence imager and probing with biomarkers specific for cathepsins (ProSense) and bone remodelling (OsteoSense). The inflammatory response was decreased considerably ($p < 0.005$) with an increased dose of CaeA (Fig. 4, *E* and *F*). Further, compared with control mice, the level of the proinflammatory cytokines IL-6, TNF-α, and IFN-γ was lower in the joint capsule of animals treated with CaeA (Fig. 4*G*).

During the early onset of disease (30 days), we also enumerated the frequency of Tregs in the draining lymph nodes. The results showed that animals treated with CaeA exhibited, *in vivo*, an increased percentage of Tregs (Fig. 4*H*). In contrast, a decline in the yield of IFN-γ and TNF-α was noticed when challenging cells with collagen *in vitro* (Fig. 4*I*). We also observed a reduction in the serum levels of matrix metalloproteinase-3 in mice that received CaeA (Fig. 4*J*). Secretion of the proinflammatory marker matrix metalloproteinase-3 has been reported to be inhibited by Tregs (35). In essence, these results (Fig. 4, *A–J*) indicate categorically that CaeA restrains arthritis symptoms by inducing the generation of Tregs and suppressing proinflammatory factors.

CaeA Specifically Interferes with STAT1 Signaling—The cytokine milieu plays an important role in the lineage commitment of CD4 T cells. Furthermore, cytokines exert signaling through a group of conserved proteins known as STATs. Hence, we next examined whether CaeA influences cytokine-mediated signaling of STATs. Interestingly, CD4 T cells preincubated with different concentrations of CaeA significantly ($p < 0.005$) inhibited the phosphorylation of STAT1 signaling mediated by IFN-γ and IL-6 (Fig. 5, *A* and *B*). To further corroborate the effect of CaeA on STAT1, we quantified the binding of STAT1 to its DNA with an enriched nuclear protein lysate of IFN-γ-treated CD4 T cells. We observed decreased STAT1 binding to DNA, substantiating the observation (Fig. 5*C*) that CaeA specifically antagonizes STAT1 signaling. The inhibitor of JAK pyradone 6, used as a positive control, also showed inhibition of STAT1 binding to DNA. No change was observed in the phosphorylation of JAK1/2 by CaeA (Fig. 5*D*). The suppressor of cytokine signaling 1 (SOCS1) expression levels were augmented with CaeA (Fig. 5*E*). SOCS1 has been reported to antagonize interferon signaling by preventing the phosphorylation of STAT1 by JAK1/2 (36, 37). We also studied the expression of IFN-dependent genes like ISG15, IRF-1, IRF-3, and IRF-7. It was observed that the levels of ISG15, IRF-1, and IRF-7 were suppressed on CaeA treatment (Fig. 5, *F–H*). No change was observed in the case of IRF-3 (data not shown). Furthermore, CaeA treatment failed to alter IL-6- and IL-12-mediated STAT3 and STAT4 signaling, respectively (Fig. 6, *A* and *B*), thus confirming the specificity of CaeA and its interference in STAT1 signaling.

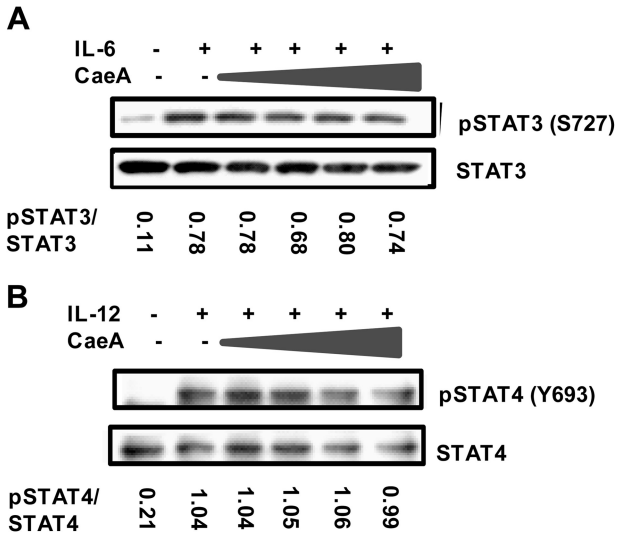

FIGURE 6. **CaeA does not operate through IL-6- and IL-12-mediated STAT3 and STAT4 signaling pathways in CD4 T cells.** CD4 T cells were treated with various concentrations of CaeA (0.04–0.31 μM) for 24 h prior to IL-6 and IL-12 stimulation (15 min). Phosphorylation of STAT3 (*A*, *pSTAT3*) and STAT4 (*B*, *pSTAT4*) was performed by Western blotting. The data in the *insets* of the images represent the fold change in phosphorylation. The results shown are from three independent experiments.

CaeA Interferes with IFN-γ Stimulation and Suppresses the Expression of FasL, Smad7, and T-bet—STAT1 is an important transcription factor for IFN-γ-mediated signaling. Because CaeA inhibits STAT1 phosphorylation, we next examined the status of IFN-γ-induced FasL, Smad7, and T-bet expression. The expression of FasL is under the control of IFN-γ-mediated STAT1 signaling (38, 39). CaeA significantly ($p < 0.05$) suppressed FasL expression (Fig. 7, *A* and *B*). RT-qPCR data depict a dose-dependent decrease in the levels of Smad7 and T-bet with CaeA treatment (Fig. 7, *C* and *D*). We further supported these results with Western blotting experiments (Fig. 7, *E* and *F*). Overall, the results of these experiments indicate that CaeA interferes with the IFN-γ-mediated signaling pathway and genes under the control of STAT1 (Fig. 7, *A–F*).

CaeA Enhances TGF-β-mediated Smad3 Signaling—TGF-β differentiates Tregs through Smad3 signaling (40). CaeA synergizes with TGF-β in the lineage commitment of Tregs (Fig. 1, *A–C*). Therefore, we studied the role of CaeA in bolstering TGF-β-mediated Smad3 signaling. CaeA significantly enhanced TGF-β induced Smad3 phosphorylation of activated CD4 T cells (Fig. 8*A*). IFN-γ inhibits TGF-β-elicited phosphorylation of Smad3 (41). However, increased TGF-β-induced Smad3 phosphorylation was noticed with CaeA treatment (Fig.

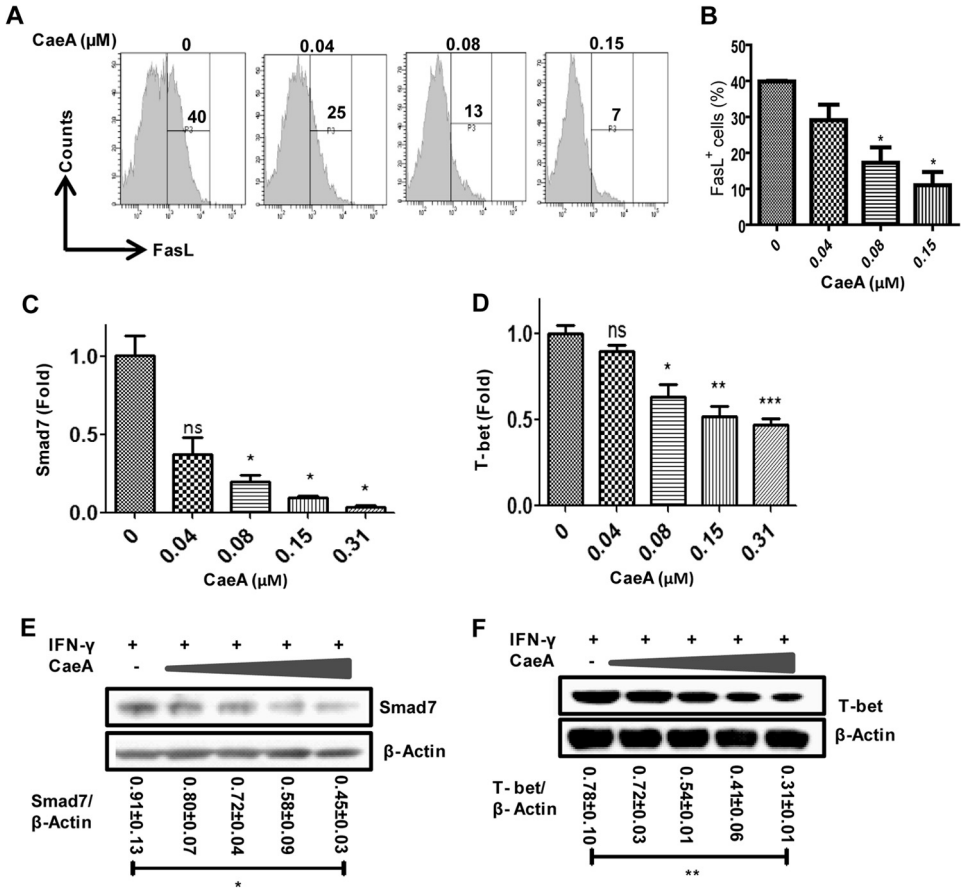

FIGURE 7. **CaeA interferes with IFN-γ treatment and suppresses FasL, Smad7, and T-bet expression.** CD4 T cells were treated with CaeA (0.04–0.31 μM) and examined for the expression of FasL, Smad7, and T-bet. *A* and *B*, flow cytometry histograms and bar graph depicting the reduced percentage of FasL$^+$ CD4 T cells. *C* and *D*, bar diagrams indicating the mean ± S.E. of the fold change expression monitored by RT-qPCR of Smad7 and T-bet, respectively. *E* and *F*, data in the *insets* of the Western blot analyses depict the fold change in the expression of Smad7 and T-bet, respectively. The results presented are from three independent experiments. *, $p \leq 0.05$; **, 0.005; ***, 0.0001; *ns*, not significant.

8*B*). This signifies categorically that CaeA neutralizes the IFN-γ effect. These results were authenticated further by nuclear translocation of Smad3 (Fig. 8*C*). SIS3 is a Smad3 inhibitor, therefore we used it as a positive control to prove the specificity of Smad3 binding to DNA (42). IFN-γ also impedes the generation of Tregs (43). Consequently, the role of CaeA in rescuing Tregs from IFN-γ-influenced suppression was studied. Remarkably, CaeA treatment significantly ($p < 0.005$) rescued the Tregs from the inhibitory effect of IFN-γ, as evidenced by an increased percentage of Foxp3$^+$ CD4 T cells (Fig. 8, *D* and *E*). We also explicitly ascertained the authenticity of CaeA-induced formation of Tregs by SIS3. The results establish categorically that the Tregs generated by CaeA are entirely dependent on Smad3 activity, as verified by a noteworthy ($p < 0.005$) retardation of Foxp3$^+$ cells (Fig. 8, *F* and *G*). Consequently, it may be concluded from the data that CaeA can neutralize the suppressive action of IFN-γ in TGF-β-mediated Smad3 signaling and, thus, helps in rescuing Tregs.

DISCUSSION

It has been reported recently that autoimmune diseases have increased considerably in the developed world (44). Furthermore, women suffer three times more than men from autoimmune diseases. Autoimmune diseases can inflict debilitating damage to body components. These diseases can influence virtually any part of the body, including the brain/nervous system (multiple sclerosis), heart (myocarditis), pancreas (type 1 diabetes), joints (rheumatoid arthritis), and multiple organs (systemic lupus erythematosus) (45). Several therapies are available for the treatment of autoimmune diseases. However, it is unfortunate that existing therapies have severe side effects (6). For example, more than 100,000 Americans are hospitalized annually because of the side effects of ulcers and gastrointestinal bleeding. As a result, 7000–10,000 of them die because of drug-inflicted injuries (46). With limited options for drug therapy, it is an urgent need and a challenge for the scientific community to identify alternative therapies that can effectively and safely control and cure autoimmune diseases.

Recently, the role of Tregs has been linked successfully to immune suppression (47–48). Further, Tregs can effectively impede the function of Th1 and Th17 cells. Th1 and Th17 cells play important role in provoking autoimmune diseases (49). Furthermore, Tregs can be generated successfully *in vitro*. Therefore, this strategy can be used as a possible remedial measure to treat autoimmune diseases. Unfortunately, such Tregs were unstable and lost their regulatory properties (32). Class-specific depletion of gut microbiota and cytophage-flavo-

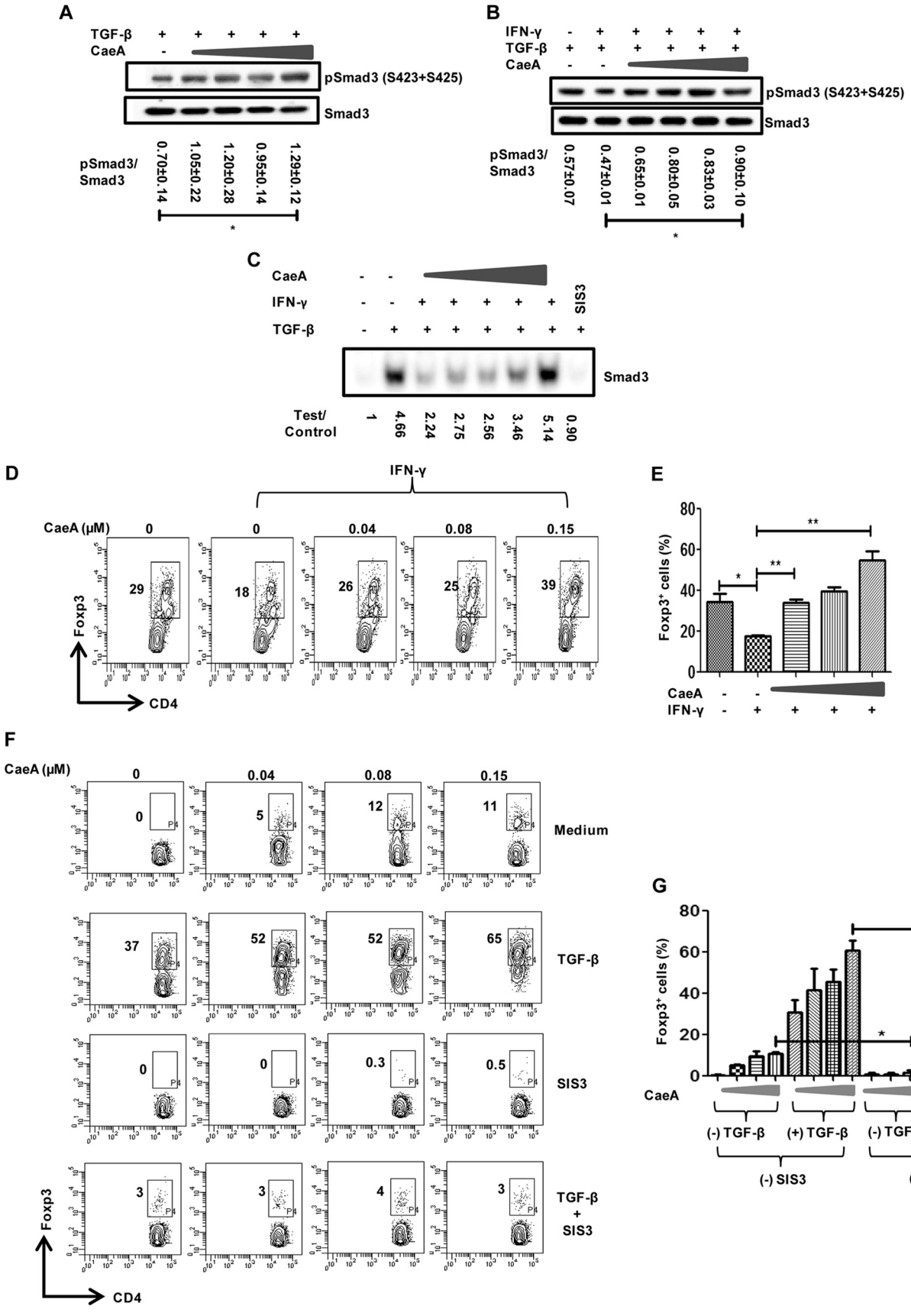

bacter-bacteroidetes by vancomycin treatment has also been known to suppress Th17 differentiation and induction of Tregs *in vivo* (50). The change in the gut microbiota also enhances the susceptibility to allergic asthma (51). Hence, a regular search is being undertaken to identify safer and better methods for generating stable Tregs (14). For this reason, we identified CaeA, which can successfully generate stable and functional Tregs *in vitro* and *in vivo*. Consequently, the following major observations were made during the study with CaeA: the induction of the generation of Tregs individually and in concert with TGF-β, the suppression of Th1 and Th17 cells, the amelioration of experimental arthritis, the inhibition of the IL-6- and IFN-γ-mediated STAT1 phosphorylation, and the augmentation of TGF-β-induced signaling of Smad3.

In this study, we demonstrated the *vis-à-vis* impact of CaeA on the generation of Tregs. Interestingly, CaeA successfully induced the formation of Tregs. Additionally, CaeA exhibited a synergism with TGF-β and further substantiated the augmentation in the pool of Tregs. We further authenticated the role of CaeA in generating Tregs by increased mitochondrial membrane potential (lipid peroxidation). It has been reported that Tregs rely on lipid peroxidation (30). Further, the presence of $CD44^{hi}$-expressing effector T cells has a negative effect on Tregs (52). However, we noticed that CaeA down-regulated CD44 on activated CD4 T cells, eventually favoring Treg generation. Furthermore, we demonstrated that cTregs were functionally competent because they inhibited the activation of effector T cells and suppressed alloreactivity.

It has been reported that gene expression elicited by cytokines can program T cell differentiation by their respective transcription factors. The cytokines IL-12+IFN-γ, TGF-β, and IL-6+TGF-β are known to favor the differentiation of naïve CD4 T cells to Th1, Tregs, and Th17, respectively (16, 53, 54). IFN-γ induces the activation of the transcription factor STAT1 through its receptor-associated protein tyrosine kinase JAK1 (55). The inhibitor for the JAK-STAT pathway, tofacitinib, is used to treat rheumatoid arthritis patients (56, 57). Suppressors of cytokine signaling (SOCS) are a special class of proteins responsible for the inhibition of cytokine signaling by preventing the phosphorylation of STATs (36). SOCS1 specifically antagonizes interferon signaling by inhibiting the phosphorylation of STAT1 (37). T-bet is a transcription factor that is strongly induced by STAT1 and is essential for the differentiation of Th1 and Th17 cells (58). IL-6 transduces the signal through the transcription factor STAT3 and also shares the STAT1 signaling pathway (59), whereas TGF-β signals through a cascade of the transcription factors Smad2, Smad3, and Smad4 (40). Hence, on the basis of these earlier findings, we next established the mechanism of action operating in the CaeA-mediated generation of Tregs. Remarkably, our results demonstrate that CaeA antagonizes the phosphorylation of the transcription factor STAT1 induced by IFN-γ and IL-6. Our results showed the enhanced expression of SOCS1 by CaeA. SOCS1 is responsible for the stabilization of Foxp3 by controlling Th1 and Th17 differentiation and suppressing STAT1 phosphorylation (60), therefore indicating that CaeA inhibits the differentiation of both Th1 cells and Th17 cells by increasing SOCS1. IFN-γ-mediated phosphorylation of STAT1 leads to the expression of T-bet, Smad7, and FasL (61, 62). Intriguingly, CaeA treatment down-regulated the exhibition of T-bet, Smad7, and FasL. It signifies that CaeA controls the expression of T-bet, Smad7, and FasL by antagonizing STAT1. It has been reported that Smad7 is responsible for the inhibition of the regulatory function of Tregs (63). Interestingly, it was noted that CaeA decreased the level of Smad7. This may be correlated with the enhanced suppressive ability of cβTregs.

The signaling events triggered by TGF-β are regulated negatively by IFN-γ (62). Phosphorylation of STAT1 induces transcription of Smad7, which is a negative regulator for the cascade of Smad3-mediated TGF-β signaling (64). Interestingly, CaeA suppressed IFN-γ induced Smad7 expression. Further, CaeA rescued inhibition of the Smad3 cascade, induced by IFN-γ-mediated Smad7 signaling. This indicates that CaeA inhibits the neutralizing effect of IFN-γ on TGF-β-mediated Smad3 signaling and, thereby, promotes the generation of Tregs. It is also known that IFN-γ induces reactive oxygen species generation, which interferes with the formation of Tregs (43). Remarkably, it was noticed that CaeA suppressed the release of reactive oxygen species and, therefore, may be supporting the generation of Tregs, even in the presence of IFN-γ (data not shown). SIS3 is an inhibitor of Smad3-mediated signaling of TGF-β. Finally, we established the specificity of CaeA-mediated Smad3 induction of the generation of Tregs by using SIS3. We noticed a significant decline in the frequency of $Foxp3^+$ Tregs. These data categorically authenticate the specificity of CaeA-induced generation of Tregs. We report here, for the first time, that suppression of IFN-γ-mediated STAT1 leads to enhanced Smad3 activity, thereby increasing the $Foxp3^+$ Treg population. In essence, our signaling data provide insights into the mechanism of action of induction of Tregs by CaeA by stimulating the Smad3 pathway.

Although Tregs are known to regulate the suppression of the immune system, this property is not very well retained *in vivo* (47, 48, 65). Furthermore, it is also known that the presence of the proinflammatory cytokines IL-6, IL-12, and IFN-γ can influence the stability of Tregs. Therefore, this may limit their application for treating autoimmunity (31–32). Hence, it was very important for us to monitor the *in vivo* stability of cTregs. Interestingly, our study revealed that cTregs were not affected by the IL-6, IL-12, and IFN-γ

FIGURE 8. **CaeA synergizes with TGF-β-mediated Smad3 signaling and rescues Tregs from IFN-γ-mediated suppression.** Naïve CD4 T cells cultured for 48 h with different concentrations of CaeA were stimulated either with anti-CD3 and CD28 Abs (*A*) or IFN-γ (*B* and *C*). *A* and *B*, cultures were pulsed with TGF-β for an additional 60 min and Western blotting was performed for Smad3 phosphorylation. *C*, nuclear translocation by EMSA. SIS3 was used as an inhibitor for Smad3. *D* and *E*, Tregs were generated in the presence of IFN-γ. The data of $Foxp3^+$ T cells represented as percent (*E*) in the *insets* of the flow cytometry contour plots and mean ± S.E. in the bar diagrams (*E*) indicate rescuing of Tregs by CaeA from IFN-γ-induced suppression of the cells. Flow cytometry contour plots (*F*) and data in the bar diagram (mean ± S.E.) (*G*) represent the decrease in the percentage of $Foxp3^+$ CD4 T cells in the presence of SIS3. *, $p < 0.05$; $p < 0.005$. Results are representative of three independent experiments.

milieu. These conditions favor the differentiation of Th17 and Th1 cells, respectively. We also demonstrated that CaeA can directly suppress the generation of Th1 and Th17 cells.

We proved the functionality of cTregs *in vivo* in an experimental model of arthritis. It is worth mentioning here that the animals treated with CaeA exhibited a significant inhibition of arthritis, as evidenced by decreased inflammation and clinical symptoms. Interestingly, these animals also showed an enhanced population of Foxp3$^+$ Tregs. Overall, our study indicates that CaeA may be a potent future immunotherapeutic agent for treating arthritis by inducing the generation of Tregs.

Acknowledgments—We thank Dr. S. Majumdar (Division of Cell Biology and Immunology, Institute of Microbial Technology (Council of Scientific and Industrial Research), Chandigarh, India) for critically evaluating the manuscript, Dr. Kim Vaiphei (Department of Histopathology, Postgraduate Institute of Medical Education and Research, Chandigarh, India) for histopathology, and Dr. Radhika Srinivas (Department of Cytology, Postgraduate Institute of Medical Education and Research) for helping with analysis of the pathology of mouse knee joints.

REFERENCES

1. Kappler, J. W., Roehm, N., and Marrack, P. (1987) T cell tolerance by clonal elimination in the thymus. *Cell* **49,** 273–280
2. Vignali, D. A., Collison, L. W., and Workman, C. J. (2008) How regulatory T cells work. *Nat. Rev. Immunol.* **8,** 523–532
3. Sakaguchi, S., Sakaguchi, N., Asano, M., Itoh, M., and Toda, M. (1995) Immunologic self-tolerance maintained by activated T cells expressing IL-2 receptor α-chains (CD25): breakdown of a single mechanism of self-tolerance causes various autoimmune diseases. *J. Immunol.* **155,** 1151–1164
4. Fathman, C. G., and Lineberry, N. B. (2007) Molecular mechanisms of CD4$^+$ T-cell anergy. *Nat. Rev. Immunol.* **7,** 599–609
5. Fathman, C. G., Soares, L., Chan, S. M., and Utz, P. J. (2005) An array of possibilities for the study of autoimmunity. *Nature* **435,** 605–611
6. Rosato, E., Pisarri, S., and Salsano, F. (2010) Current strategies for the treatment of autoimmune diseases. *J. Biol. Regul. Homeost. Agents* **24,** 251–259
7. Payne, R. (2000) Limitations of NSAIDs for pain management: toxicity or lack of efficacy? *J. Pain* **1,** 14–18
8. Masunaga, Y., Ohno, K., Ogawa, R., Hashiguchi, M., Echizen, H., and Ogata, H. (2007) Meta-analysis of risk of malignancy with immunosuppressive drugs in inflammatory bowel disease. *Ann. Pharmacother.* **41,** 21–28
9. de Mattos, A. M., Olyaei, A. J., and Bennett, W. M. (2000) Nephrotoxicity of immunosuppressive drugs: long-term consequences and challenges for the future. *Am. J. Kidney Dis.* **35,** 333–346
10. Shevach, E. M. (2004) Regulatory/suppressor T cells in health and disease. *Arthritis Rheum.* **50,** 2721–2724
11. Bluestone, J. A., and Tang, Q. (2004) Therapeutic vaccination using CD4$^+$CD25$^+$ antigen-specific regulatory T cells. *Proc. Natl. Acad. Sci. U.S.A.* **101,** 14622–14626
12. Fontenot, J. D., Gavin, M. A., and Rudensky, A. Y. (2003) Foxp3 programs the development and function of CD4$^+$CD25$^+$ regulatory T cells. *Nat. Immunol.* **4,** 330–336
13. Hori, S., Nomura, T., and Sakaguchi, S. (2003) Control of regulatory T cell development by the transcription factor Foxp3. *Science* **299,** 1057–1061
14. Zhou, X., Kong, N., Wang, J., Fan, H., Zou, H., Horwitz, D., Brand, D., Liu, Z., and Zheng, S. G. (2010) Cutting edge: all-trans retinoic acid sustains the stability and function of natural regulatory T cells in an inflammatory milieu. *J. Immunol.* **185,** 2675–2679
15. Wu, C. J., Yang, C. Y., Chen, Y. H., Chen, C. M., Chen, L. C., and Kuo, M. L. (2013) The DNA methylation inhibitor 5-azacytidine increases regulatory T cells and alleviates airway inflammation in ovalbumin-sensitized mice. *Int. Arch. Allergy Immunol.* **160,** 356–364
16. Chen, W., Jin, W., Hardegen, N., Lei, K. J., Li, L., Marinos, N., McGrady, G., and Wahl, S. M. (2003) Conversion of peripheral CD4$^+$CD25-naive T cells to CD4$^+$CD25$^+$ regulatory T cells by TGF-β induction of transcription factor Foxp3. *J. Exp. Med.* **198,** 1875–1886
17. Nadkarni, S., Mauri, C., and Ehrenstein, M. R. (2007) Anti-TNF-α therapy induces a distinct regulatory T cell population in patients with rheumatoid arthritis via TGF-β. *J. Exp. Med.* **204,** 33–39
18. Battaglia, M., Stabilini, A., and Roncarolo, M. G. (2005) Rapamycin selectively expands CD4$^+$CD25$^+$FoxP3$^+$ regulatory T cells. *Blood* **105,** 4743–4748
19. Sauer, S., Bruno, L., Hertweck, A., Finlay, D., Leleu, M., Spivakov, M., Knight, Z. A., Cobb, B. S., Cantrell, D., O'Connor, E., Shokat, K. M., Fisher, A. G., and Merkenschlager, M. (2008) T cell receptor signaling controls Foxp3 expression via PI3K, Akt, and mTOR. *Proc. Natl. Acad. Sci. U.S.A.* **105,** 7797–7802
20. Houde, V. P., Brûlé, S., Festuccia, W. T., Blanchard, P. G., Bellmann, K., Deshaies, Y., and Marette, A. (2010) Chronic rapamycin treatment causes glucose intolerance and hyperlipidemia by upregulating hepatic gluconeogenesis and impairing lipid deposition in adipose tissue. *Diabetes* **59,** 1338–1348
21. Borel, J. F. (2002) History of the discovery of cyclosporin and of its early pharmacological development. *Wien. Klin. Wochenschr.* **114,** 433–437
22. Kino, T., Hatanaka, H., Miyata, S., Inamura, N., Nishiyama, M., Yajima, T., Goto, T., Okuhara, M., Kohsaka, M., and Aoki, H. (1987) FK-506, a novel immunosuppressant isolated from a *Streptomyces*. II. Immunosuppressive effect of FK-506 *in vitro*. *J. Antibiot.* **40,** 1256–1265
23. Sehgal, S. N., Baker, H., and Vézina, C. (1975) Rapamycin (AY-22,989), a new antifungal antibiotic. II. Fermentation, isolation and characterization. *J. Antibiot.* **28,** 727–732
24. Funk, A., and Divekar, P. V. (1959) Caerulomycin, a new antibiotic from *Streptomyces caeruleus* Baldacci. I. Production, isolation, assay, and biological properties. *Can. J. Microbiol.* **5,** 317–321
25. Chatterjee, D. K., Raether, W., Iyer, N., and Ganguli, B. N. (1984) Caerulomycin, an antifungal antibiotic with marked *in vitro* and *in vivo* activity against *Entamoeba histolytica*. *Z. Parasitenkd.* **70,** 569–573
26. Collison, L. W., and Vignali, D. A. (2011) *In vitro* Treg suppression assays. *Methods Mol. Biol.* **707,** 21–37
27. Williams, R. O. (2004) Collagen-induced arthritis as a model for rheumatoid arthritis. *Methods Mol. Med.* **98,** 207–216
28. Doncarli, A., Stasiuk, L. M., Fournier, C., and Abehsira-Amar, O. (1997) Conversion *in vivo* from an early dominant Th0/Th1 response to a Th2 phenotype during the development of collagen-induced arthritis. *Eur. J. Immunol.* **27,** 1451–1458
29. Osaki, M., Tan, L., Choy, B. K., Yoshida, Y., Cheah, K. S., Auron, P. E., and Goldring, M. B. (2003) The TATA-containing core promoter of the type II collagen gene (COL2A1) is the target of interferon-γ-mediated inhibition in human chondrocytes: requirement for Stat1 α, Jak1 and Jak2. *Biochem. J.* **369,** 103–115
30. Michalek, R. D., Gerriets, V. A., Jacobs, S. R., Macintyre, A. N., MacIver, N. J., Mason, E. F., Sullivan, S. A., Nichols, A. G., and Rathmell, J. C. (2011) Cutting edge: distinct glycolytic and lipid oxidative metabolic programs are essential for effector and regulatory CD4+ T cell subsets. *J. Immunol.* **186,** 3299–3303
31. Pasare, C., and Medzhitov, R. (2003) Toll pathway-dependent blockade of CD4$^+$CD25$^+$ T cell-mediated suppression by dendritic cells. *Science* **299,** 1033–1036
32. Korn, T., Reddy, J., Gao, W., Bettelli, E., Awasthi, A., Petersen, T. R., Bäckström, B. T., Sobel, R. A., Wucherpfennig, K. W., Strom, T. B., Oukka, M., and Kuchroo, V. K. (2007) Myelin-specific regulatory T cells accumulate in the CNS but fail to control autoimmune inflammation. *Nat. Med.* **13,** 423–431
33. Damsker, J. M., Hansen, A. M., and Caspi, R. R. (2010) Th1 and Th17 cells: adversaries and collaborators. *Ann. N.Y. Acad. Sci.* **1183,** 211–221
34. Tang, Q., Henriksen, K. J., Bi, M., Finger, E. B., Szot, G., Ye, J., Masteller, E. L., McDevitt, H., Bonyhadi, M., and Bluestone, J. A. (2004) *In vitro*-expanded antigen-specific regulatory T cells suppress autoimmune diabe-

tes. *J. Exp. Med.* **199,** 1455–1465
35. Cao, Y., Xu, W., and Xiong, S. (2013) Adoptive transfer of regulatory T cells protects against Coxsackievirus B3-induced cardiac fibrosis. *PLoS ONE* **8,** e74955
36. Yoshimura, A., Naka, T., and Kubo, M. (2007) SOCS proteins, cytokine signalling and immune regulation. *Nat. Rev. Immunol.* **7,** 454–465
37. Song, M. M., and Shuai, K. (1998) The suppressor of cytokine signaling (SOCS) 1 and SOCS3 but not SOCS2 proteins inhibit interferon-mediated antiviral and antiproliferative activities. *J. Biol. Chem.* **273,** 35056–35062
38. Martins, G. A., Vieira, L. Q., Cunha, F. Q., and Silva, J. S. (1999) γ Interferon modulates CD95 (Fas) and CD95 ligand (Fas-L) expression and nitric oxide-induced apoptosis during the acute phase of *Trypanosoma cruzi* infection: a possible role in immune response control. *Infect. Immun.* **67,** 3864–3871
39. De Rose, V., Cappello, P., Sorbello, V., Ceccarini, B., Gani, F., Bosticardo, M., Fassio, S., and Novelli, F. (2004) IFN-γ inhibits the proliferation of allergen-activated T lymphocytes from atopic, asthmatic patients by inducing Fas/FasL-mediated apoptosis. *J. Leukocyte Biol.* **76,** 423–432
40. Heldin, C. H., Miyazono, K., and ten Dijke, P. (1997) TGF-β signalling from cell membrane to nucleus through SMAD proteins. *Nature* **390,** 465–471
41. Weng, H., Mertens, P. R., Gressner, A. M., and Dooley, S. (2007) IFN-γ abrogates profibrogenic TGF-β signaling in liver by targeting expression of inhibitory and receptor Smads. *J. Hepatol.* **46,** 295–303
42. Jinnin, M., Ihn, H., and Tamaki, K. (2006) Characterization of SIS3, a novel specific inhibitor of Smad3, and its effect on transforming growth factor-β1-induced extracellular matrix expression. *Mol. Pharmacol.* **69,** 597–607
43. Chang, J. H., Kim, Y. J., Han, S. H., and Kang, C. Y. (2009) IFN-γ-STAT1 signal regulates the differentiation of inducible Treg: potential role for ROS-mediated apoptosis. *Eur. J. Immunol.* **39,** 1241–1251
44. Rook, G. A. (2012) Hygiene hypothesis and autoimmune diseases. *Clin. Rev. Allergy Immunol.* **42,** 5–15
45. Davidson, A., and Diamond, B. (2001) Autoimmune diseases. *N. Engl. J. Med.* **345,** 340–350
46. Wolfe, M. M., Lichtenstein, D. R., and Singh, G. (1999) Gastrointestinal toxicity of nonsteroidal antiinflammatory drugs. *N. Engl. J. Med.* **340,** 1888–1899
47. Issa, F., and Wood, K. J. (2010) $CD4^+$ regulatory T cells in solid organ transplantation. *Curr. Opin. Organ Transplant.* **15,** 757–764
48. Morgan, M. E., Flierman, R., van Duivenvoorde, L. M., Witteveen, H. J., van Ewijk, W., van Laar, J. M., de Vries, R. R., and Toes, R. E. (2005) Effective treatment of collagen-induced arthritis by adoptive transfer of $CD25^+$ regulatory T cells. *Arthritis Rheum.* **52,** 2212–2221
49. Dardalhon, V., Korn, T., Kuchroo, V. K., and Anderson, A. C. (2008) Role of Th1 and Th17 cells in organ-specific autoimmunity. *J. Autoimmun.* **31,** 252–256
50. Ivanov, I. I., Frutos Rde, L., Manel, N., Yoshinaga, K., Rifkin, D. B., Sartor, R. B., Finlay, B. B., and Littman, D. R. (2008) Specific microbiota direct the differentiation of IL-17-producing T-helper cells in the mucosa of the small intestine. *Cell Host Microbe* **4,** 337–349
51. Russell, S. L., Gold, M. J., Hartmann, M., Willing, B. P., Thorson, L., Wlodarska, M., Gill, N., Blanchet, M. R., Mohn, W. W., McNagny, K. M., and Finlay, B. B. (2012) Early life antibiotic-driven changes in microbiota enhance susceptibility to allergic asthma. *EMBO Rep.* **13,** 440–447
52. Hill, J. A., Hall, J. A., Sun, C. M., Cai, Q., Ghyselinck, N., Chambon, P., Belkaid, Y., Mathis, D., and Benoist, C. (2008) Retinoic acid enhances Foxp3 induction indirectly by relieving inhibition from $CD4^+$CD44hi Cells. *Immunity* **29,** 758–770
53. Glimcher, L. H., and Murphy, K. M. (2000) Lineage commitment in the immune system: the T helper lymphocyte grows up. *Genes Dev.* **14,** 1693–1711
54. Bettelli, E., Carrier, Y., Gao, W., Korn, T., Strom, T. B., Oukka, M., Weiner, H. L., and Kuchroo, V. K. (2006) Reciprocal developmental pathways for the generation of pathogenic effector TH17 and regulatory T cells. *Nature* **441,** 235–238
55. Ihle, J. N. (1995) Cytokine receptor signalling. *Nature* **377,** 591–594
56. Garber, K. (2011) Pfizer's JAK inhibitor sails through phase 3 in rheumatoid arthritis. *Nat. Biotechnol.* **29,** 467–468
57. Garber, K. (2013) Pfizer's first-in-class JAK inhibitor pricey for rheumatoid arthritis market. *Nat. Biotechnol.* **31,** 3–4
58. Yang, Y., Weiner, J., Liu, Y., Smith, A. J., Huss, D. J., Winger, R., Peng, H., Cravens, P. D., Racke, M. K., and Lovett-Racke, A. E. (2009) T-bet is essential for encephalitogenicity of both Th1 and Th17 cells. *J. Exp. Med.* **206,** 1549–1564
59. Croker, B. A., Krebs, D. L., Zhang, J. G., Wormald, S., Willson, T. A., Stanley, E. G., Robb, L., Greenhalgh, C. J., Förster, I., Clausen, B. E., Nicola, N. A., Metcalf, D., Hilton, D. J., Roberts, A. W., and Alexander, W. S. (2003) SOCS3 negatively regulates IL-6 signaling *in vivo*. *Nat. Immunol.* **4,** 540–545
60. Takahashi, R., Nishimoto, S., Muto, G., Sekiya, T., Tamiya, T., Kimura, A., Morita, R., Asakawa, M., Chinen, T., and Yoshimura, A. (2011) SOCS1 is essential for regulatory T cell functions by preventing loss of Foxp3 expression as well as IFN-γ and IL-17A production. *J. Exp. Med.* **208,** 2055–2067
61. Lighvani, A. A., Frucht, D. M., Jankovic, D., Yamane, H., Aliberti, J., Hissong, B. D., Nguyen, B. V., Gadina, M., Sher, A., Paul, W. E., and O'Shea, J. J. (2001) T-bet is rapidly induced by interferon-gamma in lymphoid and myeloid cells. *Proc. Natl. Acad. Sci. U.S.A.* **98,** 15137–15142
62. Ulloa, L., Doody, J., and Massagué, J. (1999) Inhibition of transforming growth factor-β/SMAD signalling by the interferon-γ/STAT pathway. *Nature* **397,** 710–713
63. Mizobuchi, T., Yasufuku, K., Zheng, Y., Haque, M. A., Heidler, K. M., Woods, K., Smith, G. N., Jr., Cummings, O. W., Fujisawa, T., Blum, J. S., and Wilkes, D. S. (2003) Differential expression of Smad7 transcripts identifies the $CD4^+$CD45RChigh regulatory T cells that mediate type V collagen-induced tolerance to lung allografts. *J. Immunol.* **171,** 1140–1147
64. Dooley, S., Hamzavi, J., Breitkopf, K., Wiercinska, E., Said, H. M., Lorenzen, J., Ten Dijke, P., and Gressner, A. M. (2003) Smad7 prevents activation of hepatic stellate cells and liver fibrosis in rats. *Gastroenterology* **125,** 178–191
65. Bagavant, H., and Tung, K. S. (2005) Failure of $CD25^+$ T cells from lupus-prone mice to suppress lupus glomerulonephritis and sialoadenitis. *J. Immunol.* **175,** 944–950

Caerulomycin A Enhances Transforming Growth Factor-β (TGF-β)-Smad3 Protein Signaling by Suppressing Interferon- γ (IFN-γ)-Signal Transducer and Activator of Transcription 1 (STAT1) Protein Signaling to Expand Regulatory T Cells (Tregs)

Rama Krishna Gurram, Weshely Kujur, Sudeep K. Maurya and Javed N. Agrewala

J. Biol. Chem. 2014, 289:17515-17528.
doi: 10.1074/jbc.M113.545871 originally published online May 8, 2014
